

SAND095-16356

Symposium on Thermal Sciences and Engineering in Honor  
of Chancellor Chang-Lin Tien, November 1995WIND-INDUCED INTERACTION OF A LARGE CYLINDRICAL  
CALORIMETER AND AN ENGULFING JP-8 POOL FIRE<sup>†</sup>Louis A. Gritzo\*, Vernon F. Nicolette\*, Douglas Murray\*\*, Jaime L. Moya\*\*\*,  
Russell D. Skocynec\*

\*Thermal and Fluid Engineering, Department 1513, MS 0835

\*\*Thermal Characterization and Simulation, Department 2735, MS 1135  
Sandia National Laboratories  
Albuquerque, New Mexico

## ABSTRACT

As part of a research program in fire science and technology at Sandia National Laboratories (SNL), an experimental and computational investigation of the fire phenomenology associated with the presence of a large (3.66 m diameter), fuselage-sized cylindrical calorimeter engulfed in a large (18.9 m diameter) JP-8 pool fire subjected to high (10.2 m/s) winds was performed.

The conditions investigated here resulted in a twofold increase in the incident heat flux to the surface of the object relative to heat fluxes typical of large hydrocarbon fires without engulfed objects. Due to the enhanced fuel/air mixing, enhanced turbulence, and larger flame volume, the highest heat fluxes are observed on the leeward side of the calorimeter. Radiative heat fluxes of 150-250 kW/m<sup>2</sup> on this side, with the maximum heat flux occurring near the top of the calorimeter, were measured. Radiative heat fluxes of 60-200 kW/m<sup>2</sup> were measured on the windward side, with the highest heat flux near the bottom of the calorimeter. Measured and predicted heat fluxes to the pool surface of 25-90 kW/m<sup>2</sup> were observed. The presence of the calorimeter tends to decrease the overall fuel consumption rate primarily due to redirection of the flame zone away from the pool surface. Overall, the numerical model does a reasonable job of representing the essential features of the fire environment but under predicts the heat flux to the calorimeter.

These results emphasize the importance of considering the wind-induced interaction of fires and large objects when estimating the incident heat fluxes on an engulfed object. These measurements and analyses are of particular interest since few studies to date have addressed cases where the fire and object are of comparable size.

<sup>†</sup>This work was sponsored by the Defense Nuclear Agency Weapons System Safety Assessment and Fuel Fire Testbase Programs and was performed in part at Sandia National Laboratories under United States Department of Energy contract DE AC04-94 AL85000.

## INTRODUCTION

Large-fire characterization and simulation is a primary objective of the fire science and technology research program at SNL. The development of predictive fire field models and simplified, deterministic Risk Assessment Compatible Fire Models (RACFMs) is tightly coupled with a full-scale fuel fire test program. Gaining an understanding of large-fire phenomenology, including the effects of wind and the influence of large structures engulfed by, or adjacent to, the continuous flame zone is central to this effort. This understanding forms the foundation of the ability to numerically simulate large-fire environments.

Although many studies have been performed on fire phenomenology in small-scale pool fires, including contributions by Alger et al (1979) and Hamins et al. (1994), a limited number of large-scale fire phenomenology studies appear in the literature. Included in these studies are works by Johnson et al. (1982) and Gritzo et al. (1995a) which focus on the behavior of large fires without engulfed objects. Fewer studies have been performed which consider the effect of objects where the size of the object is comparable with the size of the fuel pool. Previous studies including work on fire-induced fuselage burnthrough by Sarkos, et al. (1990) and under-wing pool fires by Keltner, et al. (1994) address the scenario where the fire is small compared to the structure of interest. Small objects in large fires have been investigated experimentally by Russell and Canfield (1973) and Gregory et al. (1989).

Cases where the fire and object are of comparable size are difficult to address due to the alteration of the flow field and the related influence on the fire physics due to the presence of the object. The influence of the altered flow field on the fire physics must be known to determine the flame zone geometry and the temperature, radiative property, and velocity fields within the flame zone. Very few detailed studies within this class of problems appear in the literature. A recent contribution is the experimental study of a large, flat surface adjacent to a large fire by Gritzo, et al. (1995b). These scenarios are often of interest due to the occurrence of large fires

MASTER

## **DISCLAIMER**

This report was prepared as an account of work sponsored by an agency of the United States Government. Neither the United States Government nor any agency thereof, nor any of their employees, makes any warranty, express or implied, or assumes any legal liability or responsibility for the accuracy, completeness, or usefulness of any information, apparatus, product, or process disclosed, or represents that its use would not infringe privately owned rights. Reference herein to any specific commercial product, process, or service by trade name, trademark, manufacturer, or otherwise does not necessarily constitute or imply its endorsement, recommendation, or favoring by the United States Government or any agency thereof. The views and opinions of authors expressed herein do not necessarily state or reflect those of the United States Government or any agency thereof.

## **DISCLAIMER**

**Portions of this document may be illegible  
in electronic image products. Images are  
produced from the best available original  
document.**

which engulf objects containing personnel, weapon systems, or hazardous materials. Large aviation fuel fires which engulf an aircraft fuselage, posing a significant hazard to the occupants and cargo, are included in this class. Accordingly, an experimental and computational investigation of the fire phenomenology associated with the presence of a large (3.66 m diameter), fuselage-sized cylindrical calorimeter engulfed in a large (18.9 m diameter) JP-8 pool fire is performed here.

The test of interest in this work was conducted as part of a series of ongoing full-scale large-fire experiments at the Naval Air Weapons Center (NAWC). The objectives of this test program include supplying data required to: 1) gain a better understanding of fire phenomenology, 2) assist in continuing fire field model code validation and development, and 3) provide unique temperature and incident heat flux distributions for credible large-scale fire scenarios. Data acquired for these purposes, along with an analysis of these data, are presented in this study.

Additional insight into fire phenomenology is provided by simulations from numerical fire field models. These models predict the fire environment and hence are capable of representing changes in the flame zone due to the presence of objects. Such models are presently under development by several research organizations, including a collaborative effort established between Sandia National Laboratories (SNL) and the Norwegian Institute of Technology (NTB)/SINTEF. Results and analyses of numerical simulations are included here and are compared with observations of fire phenomena from the experimental data.

#### DESCRIPTION OF THE EXPERIMENT

The test was conducted at the CT-4 Safety Test Facility of the Naval Air Warfare Center Weapons Division China Lake, California using a 18.9 meter diameter fuel fire pool. A 3.66 meter diameter, 20 m long steel culvert section was used to form a fuselage-sized cylindrical calorimeter. The calorimeter was positioned slightly above the fuel surface with the axis of the cylinder normal to the prevailing wind direction at the facility. The test fixture was located such that the leeward edge of the mock fuselage was tangent with the leeward edge of the pool as shown in Figure 1. The interior of the calorimeter was covered with a 5 cm thick layer of ceramic fiber insulation.

Total instrumentation for the test consisted of 281 type-K, inconel-sheathed, ungrounded-junction thermocouples and 133 hemispherical heat flux gauges (HFGs). HFGs use a large (6 cm) diameter, thin (0.02 mm) flat sensor surface with a thermocouple attached to the interior side. The sensor surface is thermally isolated from the remainder of the gauge and hence rapidly (limited by the time constant of the thermocouple) comes to equilibrium with the fire environment. A Pyromark™ black coating is applied to yield a diffuse and gray sensor surface. When convection is negligible, (as is typical for large fires) the emissive power of the diffuse, gray sensor surface, in equilibrium with the surroundings, provides a measurement of the incident heat flux. Uncertainty of +/- 20%, depending on conditions, is estimated for these gauges.

The temperature distribution on the calorimeter was measured by attaching thermocouples to the interior of the test section at 56 locations. Heat flux to the surface of the calorimeter was measured

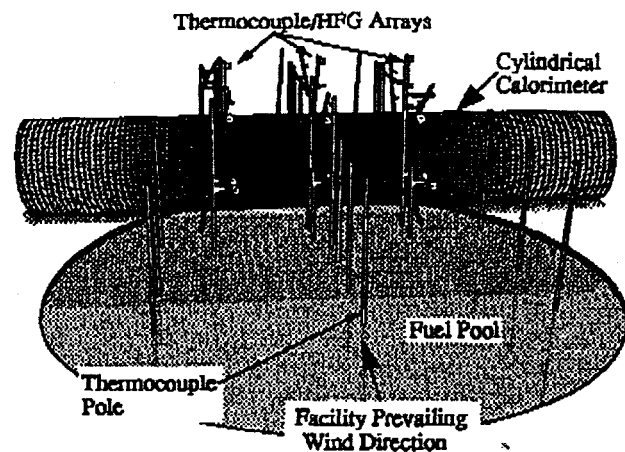


FIGURE 1: POSITION OF TEST FIXTURE, FUEL POOL AND TEST INSTRUMENTATION

by locating 38 HFGs at 5 axial and 8 radial positions such that the sensor surface was even with the exterior of the calorimeter. To characterize the fire in the vicinity of the test section, 120 thermocouples and 75 HFGs were positioned on arrays that protruded outward from the calorimeter surface at 3 axial positions and 8 radial locations. To assist in characterizing the entire continuous flame zone, thermocouples were positioned at five elevations on 17 poles which were placed within the fuel pool and where flame coverage was anticipated on the leeward side of the mock fuselage. Spatial and temporal measurements of heat flux to the pool surface were obtained by positioning upward facing HFGs at 20 locations in the pool and on the leeward side of the mock fuselage.

Incident winds were characterized with vane-type gauges. Measurements at 3 elevations were obtained at two locations 30° on either side of the facility prevailing wind direction at a distance 30 meters from the edge of the pool.

The test of interest in this study was performed by floating 14.78 m<sup>3</sup> of JP-8 aviation fuel on top of a 15 cm thick layer of water. Winds were stable during the test. An average wind speed of 10.2 m/s at an average direction 23° from the normal to the axis of the cylindrical calorimeter was measured at the 10 m elevation. Several other tests were performed as part of this series. However, this test produced very high temperatures (> 1665 K), melting inconel thermocouples and the inconel wires used to secure insulation to the test fixtures. Although the test fixture had been used for several previous tests without significant heating of the support assembly, sufficient thermal insult was experienced during this test to cause the test fixture to sag slightly during the experiment.

Approximately 100 s was required for the flame to spread across the pool. This number is primarily a qualitative measure of flame spread since 0.095 m<sup>3</sup> of gasoline was used as an accelerant. Temperatures representative of thermocouples exposed to flame sheets were observed at elevations of 0.3 m and 0.92 m in the center of the pool 62 s after ignition. The data show that full burning

(i.e. appropriate temperatures at all elevations) at the pool center was not obtained until 125 s after ignition. Thermocouples located near the pool surface on the leeward side of the mock fuselage ground indicated full burning 100 s after ignition. Towards the end of the test, the fuel was carried by the wind to the leeward end of the pool. Full burning ended at the center of the pool 697 s after ignition and there was no evidence of burning at the pool center at 715 s. On the leeward side of the pool, both full burning and all burning end approximately 930 s after ignition. These estimates of burn times, along with the corresponding average fuel consumption rate estimates, are summarized in Table 1.

TABLE 1: BURN TIME AND AVERAGE FUEL CONSUMPTION RATE ESTIMATES

Burn Time (s)			Consumption Rate <sup>a</sup> (kg/m <sup>2</sup> ·s)		
Min.	Max.	Nom.	Max.	Min.	Nom.
575	930	693	0.074	0.046	0.061

a. 14.78 m<sup>3</sup> of JP-8 consumed, JP-8 density = 808 kg/m<sup>3</sup>.

## EXPERIMENTAL RESULTS

Fuel consumption rate estimates for this test are comparable to results from previous (Gritzo et al., 1995a) JP-8 fires of the same diameter, but without objects and for significantly lower (5.5 m/s) wind speeds. In general, the fuel consumption rate increases with increasing wind speed. This trend is due to two phenomena: 1) enhanced convective mass transfer at the fuel surface, and 2) improved mixing close to the fuel surface which results in improved combustion and hence increased radiative heating of the fuel. Data from this test tend to show that the presence of an object reduces the fuel consumption rate.

Additional insight into this reduction in fuel consumption rate is provided by the time-averaged (300-600 s after ignition) heat flux to the fuel surface measurements given in Figure 2. As expected based on the measurements of fuel consumption rate, a similar overall range (25-90 kW/m<sup>2</sup>) of heat fluxes is observed between the results in Figure 2 and those of the previous (Gritzo et al., 1995a) JP-8 fire without objects subjected to 5.5 m/s winds. The influence of the calorimeter is clearly evident in the contours shown in Figure 2. A region of low heat flux near the leading edge, indicative of thin flame cover, is observed on the windward side of the fuel pool. An increase in heat flux occurs towards the pool center, forming a band of 55-60 kW/m<sup>2</sup> heat fluxes windward of the cylinder. This trend is consistent with the redirection of the plume away from the fuel surface due to the presence on the calorimeter. A small region of high heat flux along the pool centerline, potentially due to enhanced mixing at the leading edge of the pool, can be seen on the windward side of this band. An area of reduced heat flux is observed within this band immediately windward of the cylinder. This area includes a region of very low (25 kW/m<sup>2</sup>) heat flux on the windward side of the wind component parallel to the cylinder axis (i.e. the axial wind component). Reduced heat fluxes in this area are indicative of an oxygen-starved flame interface.

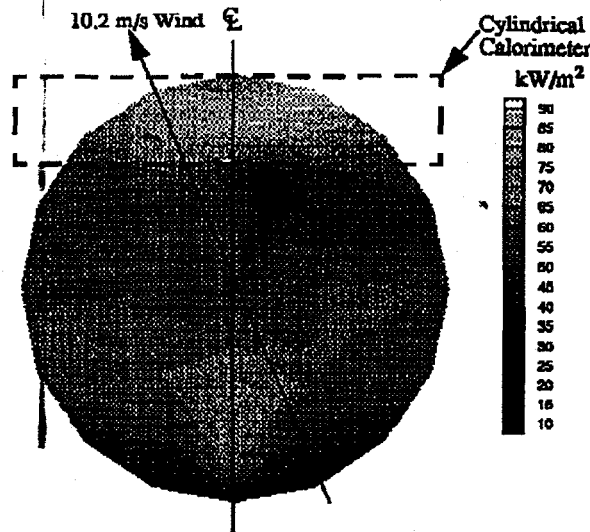


FIGURE 2: MEASURED INCIDENT HEAT FLUX TO FUEL SURFACE

rior. The highest heat fluxes are observed immediately below the cylinder in a region which is skewed slightly to the right of the pool centerline. High heat fluxes in this region are consistent with improved mixing, and hence enhanced volumetric heat release, in the accelerated flow between the cylinder and the fuel and the formation of large, well-mixed, columnar vortical structures on the leeward side of the object.

Corresponding time-averaged incident radiative heat fluxes on the surface of the cylindrical calorimeter are shown in Figure 3. Similar circumferential variations in heat flux are observed at three axial positions on the calorimeter. At each position, the minimum heat flux was measured at the top of the cylinder. This trend is consistent with the thin flame cover on the top of the cylinder observed in the video record. Increased flame cover, and enhanced mixing in the form of large, columnar vortices, were observed in the video record on the leeward side of the cylinder. Due to the enhanced air entrainment and improved mixing produced by these structures, the largest heat fluxes were measured at circumferential locations greater than 225°, i.e. on the leeward side of the calorimeter.

Although significantly less variation in incident heat flux is observed along the axis of the cylinder, the trends evident in the data are consistent with those shown in Figure 2, and illustrate the coupled interaction of the cylinder and the fire. At radial positions between 0 to 180°, increasing heat fluxes were measured along the negative x direction (i.e. in the direction of the axial wind component). This trend is consistent with the variation in heat flux to the pool observed in Figure 2 and emphasizes the influence on the axial component of the wind in directing the flame cover towards the side of the cylinder for which  $x < 0$ . On the leeward side of the cylinder, the highest heat flux was, in contrast, measured at  $x = 3.66$  m where a large columnar vortex was observed. This location also corresponds to the region of maximum heat flux to the pool surface given in Figure 2. The results presented here therefore

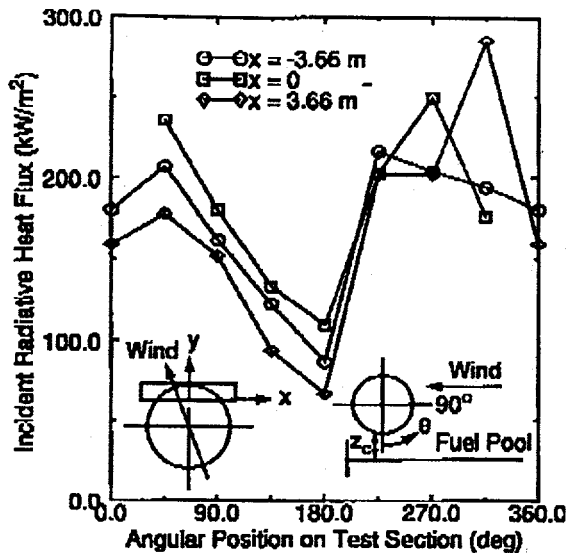


FIGURE 3: MEASURED INCIDENT HEAT FLUX TO CALORIMETER SURFACE

emphasize the influence of the wind, and the influence of large-scale turbulent structures on the distribution of heat flux to the fuel surface and to an engulfed object.

Overall, incident heat fluxes to the surface of the calorimeter are approximately twice the magnitude of those measured to the fuel surface. Potential explanations for this trend include: cooling of the local participating media near the fuel surface due to the presence of a cold fuel boundary, "blockage" of incident heat flux to the fuel surface by the fuel vapor (as investigated by Brosmer and Tien, 1987), cooling of the gauge sensor surface by the waves within the fuel, and enhanced combustion due to turbulent mixing in the viscous boundary layer adjacent to the surface of the calorimeter. Future studies are required to resolve these phenomena.

It is important to note that, in addition to the trends inherent in these results, the magnitude of the heat fluxes measured here are significantly larger than those typical of hydrocarbon fuel fires. Incident heat fluxes from 100-150 kW/m<sup>2</sup> are generally expected (Russell and Canfield, 1973, Gregory et al., 1989, and Keltner, et al., 1994) in fires where heavy hydrocarbons are the primary fuel. The unique nature of this experiment, i.e. a large object in a large fire under high winds, and the resulting influence on the flowfield and fire physics are expected to have produced the very high (> 250 kW/m<sup>2</sup>) heat fluxes observed here.

#### NUMERICAL MODEL

A fire field model (based on Kameleon Fire, Holen et al., 1990) under joint development at Sandia National Laboratories and SINTEF/NTH was used to simulate the test setup and conditions. The numerical model uses the standard k-epsilon turbulence model (with standard constants) and the Eddy Dissipation Concept combustion model (Magnussen, et al., 1979). The Discrete Transfer radiation model (Shah, 1979) is employed to calculate the thermal radiation from soot and combustion gases to the pool and to the

object. The SIMPLEC technique (Patankar and Spalding, 1982) is employed to solve the system of equations.

A spatially non-uniform Cartesian grid of 42x40x30 (high) cells was employed to model a physical domain of 150 m x 150 m x 60 m (high), with cells clustered near the object and the pool surface. Pressure boundary conditions were applied along the top of the domain, and along the two faces of the domain that were down wind. Along the two upwind boundaries, constant wind velocities were specified as 9.5 m/s for the plane normal to the cylinder, and 3.84 m/s tangent to the cylinder, both at a vertical elevation of 10 m above the ground. The velocity distribution as a function of elevation was then fitted to a logarithmic atmospheric boundary layer profile. To investigate the influence of the test fixture "sagging" during the test, the bottom of the cylindrical object was placed at two different elevations,  $z_c$ , for the calculations: the low elevation ( $z_c = 0.23$  m) was based on measurements of the cylinder elevation after the test series. The second elevation ( $z_c = 0.6$  m) was based on the nominal location of the cylinder bottom prior to the first test. The transient response of the object was modeled assuming a 0.0016 m thick wall with the properties of 1010 steel. An emissivity of 0.95 was assigned to the object to account for oxidation and soot deposition effects. The fuel evaporation rate from the pool was calculated by the model as a function of time and location, based on the local absorbed radiative heat flux. The thermo-physical properties of JP-8 fuel (Handbook of Aviation Fuel Properties, 1983) were assigned to the pool, assuming a pool thickness of 0.167 m (to include the effects of the water substrate) and a fuel absorptivity of 0.85. A 0.1 m high thin non-conducting wall was placed around the pool in the calculations to represent the lip around the fuel pool.

#### NUMERICAL RESULTS

Numerical results were obtained and analyzed at a time period corresponding to the steady wind portion of the test. The effect of the wind is to move the majority of the flame volume towards the leeward side, even though the fuel pool lies completely windward of (or directly underneath) the calorimeter. The top, windward quadrant of the cylinder (relative to the component of the wind normal to the axis of the cylinder) has the least flame coverage, while the leeward half of the cylinder has the most flame coverage. These results are consistent with observations from the video record and the measured heat flux distribution which shows a minimum in the incident radiative flux at the top of the calorimeter.

A comparison of the results for both elevations illustrates a high sensitivity of the solution to the elevation of the cylinder. The primary difference is the extent to which the flame cover is shifted to the leeward side of the object. Based on a preliminary comparison with experimental data, and the available information on the elevation of the test fixture during the majority of the test, results presented here are limited to those from the simulation at the low elevation ( $z_c = 0.23$  m).

A contour plot of the instantaneous radiative heat flux to the fuel surface for the calorimeter in the low position is shown in Figure 4. The model predicts the general trend and many of the essential features of the heat flux distribution measurements given in Figure 2. The model results, in agreement with the experimen-

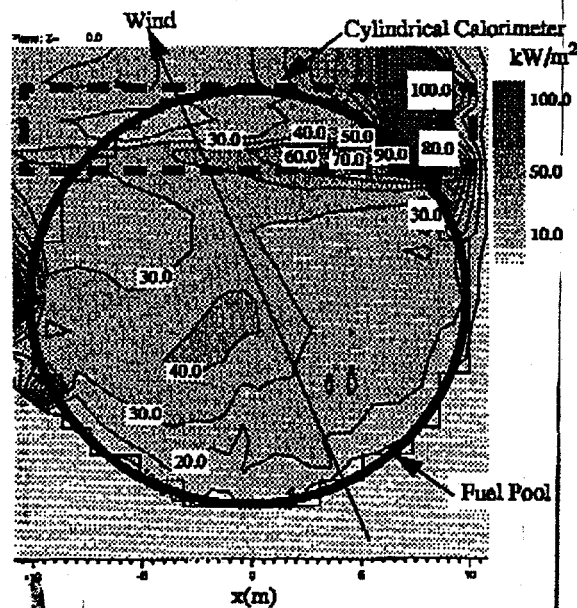


FIGURE 4: PREDICTED INCIDENT HEAT FLUX TO FUEL SURFACE

data, exhibit a "band" of reduced heat fluxes through the center of the fuel pool just windward of the calorimeter. Two regions of low heat flux within this band, one either side of the wind vector, are also evident in both the experimental data and the model predictions. A small region of increased heat flux along the pool centerline near the windward edge of the pool and the small area of low ( $\sim 10 \text{ kW/m}^2$ ) heat fluxes at the leading edge are also predicted by the model in agreement with the measurements given in Figure 2. The model also predicts a region of maximum heat flux underneath the cylinder. This region is slightly further to the right (i.e. in the windward direction of wind component parallel to the cylinder axis) than shown in Figure 2. Comparable heat fluxes ( $\sim 90 \text{ kW/m}^2$ ) are given by the model predictions and the measurements within this region, although elsewhere in the domain the measured heat fluxes tend to be greater than those predicted by the model.

The numerical model allows further investigation of the temperature and velocity field in the neighborhood of the calorimeter. A cross section of time-averaged temperatures, with superimposed velocity vectors, normal to the z-axis at an elevation of approximately 1.125 m is shown in Figure 5. A large, high temperature recirculating region, indicative of a columnar vortex which extends down to the pool surface, is clearly evident on the leeward side of the cylinder at a location corresponding to the region of maximum heat flux to the pool surface. The model therefore predicts the formation of the appropriate stable turbulent structures. Temperatures greater than 1200 K are predicted by the model within this region. Temperatures of approximately 1200 K are predicted over a large area on the windward side of the calorimeter. The blackbody heat flux at these temperatures is approxi-

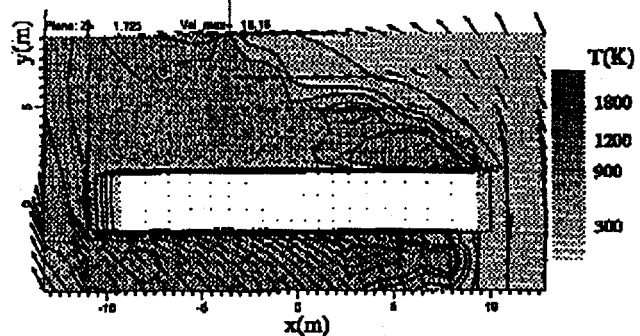


FIGURE 5: PREDICTED TEMPERATURE AND VELOCITY DISTRIBUTION

mately  $120 \text{ kW/m}^2$ , which is significantly lower than the measured heat fluxes on the surface of the calorimeter.

Instantaneous results of total radiative heat flux given in Figure 6 illustrate the presence of a region of high ( $>250 \text{ kW/m}^2$ ) heat flux at the location corresponding to the recirculation zone. The location and magnitude of this high heat flux region agree well with the experimental results presented in Figure 3. Heat fluxes over the remainder of the leeward side of the calorimeter are, in general, lower than those measured during the test. Due to the nonlinearities inherent in radiative heat transfer, the presence of such high heat flux regions can not be identified based on observations of time-averaged temperatures. Efforts to appropriately time-average radiative heat fluxes are underway.

Overall, the model does a reasonable job of representing the essential features of the fire environment. The ability to predict the recirculation zone and the associated high temperature region are encouraging. Given the assumptions inherent in the model, one expects to be able to predict turbulent structures that are stable with time. In this case, the presence of a "wake" on the leeward side of the object due to the wind, coupled with the asymmetry in air entrainment induced by the presence of the calorimeter appear to support this stable recirculation zone. Enhanced recirculation results in an increase in the ability of the flame zone to entrain air and mix the air with the fuel on the small scale. This increase in small-scale mixing is the key to achieving enhanced combustion efficiency and accordingly the ability to generate high temperatures which result in high heat fluxes within large fires. The abil-

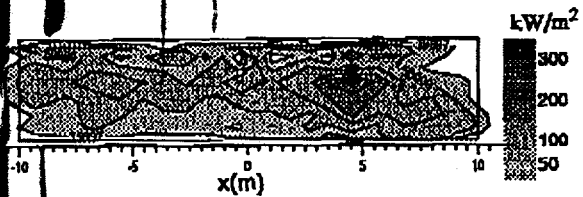


FIGURE 6: PREDICTED INCIDENT HEAT FLUX ON LEeward SIDE OF CALORIMETER

ity to identify such regions is a necessary first step in the thorough simulation of a fire environment.

Calculated pool mass loss rates (instantaneous) were generally  $0.085 \pm 0.010 \text{ kg/m}^2\text{-s}$ . This range is significantly higher than the maximum average fuel consumption rate inferred from the test results ( $0.074 \text{ kg/m}^2\text{-s}$ ). The discrepancy may result because the test results include the time period when the pool is relatively cold (which can result in lower fuel evaporation rates). Potential improvements in the fuel thermal response and evaporation rate submodels are presently being investigated. The effect of wind on mixing within the fuel pool is the principle challenge in this development.

## CONCLUSIONS

The experimental measurements, numerical simulation results, and accompanying analysis presented here emphasize the importance of the interaction between objects and the fire environment. This interaction is particularly relevant when the object and fuel pool sizes are comparable. As illustrated here, the influence of wind in these cases has a pronounced effect on the nature of the flowfield. Air entrainment and mixing are significantly enhanced, which results in increasing media temperatures, in part due to the formation of large-scale stable columnar vortices. In the case investigated here, this increase in temperature results in approximately a twofold increase in the incident heat flux to the surface of the object relative to heat fluxes typical of large, hydrocarbon fuel fires.

The following specific conclusions are presented as a result of this study:

- Temperatures sufficient to melt inconel ( $>1665 \text{ K}$ ) were observed on the leeward side of the cylindrical calorimeter under high (10.2 m/s) winds.
- The presence of a large object tends to reduce the fuel consumption rate due to the redirection of the flame zone away from the fuel surface.
- For these conditions, the minimum heat flux was observed on the top of the cylinder due to thin flame cover.
- For these conditions, the maximum heat flux to the cylinder occurs on the leeward side where a large columnar vortex was observed in both the test and the numerical simulation.
- The maximum radiative heat flux to the pool surface occurs underneath, and slightly on the leeward side, of the cylinder.
- The measured heat fluxes to the fuel surface are approximately 50% of those measured on the surface of the calorimeter.
- The numerical simulation successfully captures the formation of the major time-stable turbulent structures.
- The general trend, and some of the essential features of the heat flux distribution measurements were predicted by the numerical simulation.

Additional analytical and experimental work to obtain a more detailed understanding of the interaction of large objects in large fires is presently underway. The improved understanding of fire phenomena gained from this and other studies is critical to the

development of predictive numerical simulation tools with the ultimate goal of achieving improved fire safety.

## REFERENCES

Alger, R.S., Corlett, R.C., Gordon, A.S., and Williams, F.A., 1979, "Some Aspects of Structures of Turbulent Pool Fires," *Fire Technology*, Vol. 15, pp.142-156.

Brosmer, M., and Tien, C. L., 1987, "Radiative Energy Blockage in Large Pool Fires", *Combustion Science and Technology*, Vol. 51, pp. 21-37.

Gregory, J., Keltner, N. R., Mata, R., 1989, "Thermal Measurements in Large Pool Fires," *Journal of Heat Transfer*, vol 111, p. 446-454.

Gritzo, L. A., Nicolette, V. F., Tieszen, S. R., Moya, J. L., and Holen, J., 1995a, "Heat Transfer to the Fuel Surface in Large Pool Fires," *Transport Phenomena in Combustion*, S. H. Chan, ed., Taylor and Francis, Washington, D.C.

Gritzo, L. A., Moya, J. L., Nicolette, V. F., and Gililand, J., 1995b, "Characterization of Large JP4 Pool Fires and Heat Fluxes Incident on an Adjacent Flat Surface" to be presented at the 1995 International Conference on Fire Research and Engineering, Orlando, Florida, September 11-15.

Hamins, A., Fischer, J., Kashiwagi, T., Klassen, M. E. and Gore, J. P., 1994, "Heat Feedback to the Fuel Surface in Pool Fires," *Combustion Science and Technology*, Vol 97, pp. 37-62.

Handbook of Aviation Fuel Properties, 1983, Coordinating Research Council, Inc., Atlanta, Georgia, CRC Report No. 530.

Holen, J., Brostrom, M., and Magnussen, B. F., 1990, "Finite Difference Calculation of Pool Fires," *Proceedings of the 23rd International Symposium on Combustion*, The Combustion Institute, pp. 1677-1683.

Keltner, N. R., Gill, W. and Kent, L. A., 1994, "Simulating Fuel Spill Fires Under the Wing of an Aircraft" Fire Safety Science, proceedings of the 4th International Symposium, Kashiwagi, T. ed., Ottawa, Ontario, Canada, p. 1017-1028.

Magnussen, B. F., Hjertager, B. H., Olsen, J. G., and Bhandari, D., 1979, "The Eddy Dissipation Concept," *Proceedings of the 17th International Symposium on Combustion*, The Combustion Institute, pp. 1383-1398.

Patankar, S. V., and Spalding, D. B., 1982, "A Calculation Procedure for Heat, Mass, and Momentum Transfer in Three-dimensional Parabolic Flow," *International Journal of Heat and Mass Transfer*, vol 15, p. 1787.

Russell, L. H. and Canfield, J. A., 1973, "Experimental Measurement of Heat Transfer to a Cylinder Immersed in a Large Aviation-Fuel Fire," *Journal of Heat Transfer*, vol 95C, p. 397-407.

Sarkos, C., Webster, H., Geyer, G., Do, D., Wright, J., Collins, J., and Hampton, L., 1990, "Full-Scale Fuselage Burnthrough Tests," presented at The European Cabin Safety Conference, Gatwick International Airport, Sussex, United Kingdom, September 18-21.

Shah, N. G., 1979, "The Computation of Radiation Heat Transfer," Ph.D. thesis, University of London, Faculty of Engineering.